Diffusion of Monolayer Adatom and Vacancy Clusters: Langevin Analysis and Monte Carlo Simulations of their Brownian Motion

S. V. Khare, N. C. Bartelt, and T. L. Einstein

Department of Physics, University of Maryland, College Park, Maryland 20742-4111
(Received 10 May 1995)

In recent observations of Brownian motion of islands of adsorbed atoms and of vacancies with mean radius R, the cluster diffusion constant varies as R^{-1} and R^{-2}. From an analytical Langevin description of the cluster's steplike boundary, we find three cases, R^{-1}, R^{-2}, and R^{-3}, corresponding to the three microscopic surface mass-transport mechanisms of straight steps. We thereby provide a unified treatment of the dynamics of steps and of clusters. For corroboration, we perform Monte Carlo simulations of simple lattice gases and derive atomistic diffusion constants.

Characterizing the mechanisms of atomic mass transport on surfaces is crucial to the understanding of many important processes, such as epitaxial growth. A notable manifestation of surface transport is the diffusion of clusters [1–5]. Of the few experimental studies relating the cluster diffusion to the island size, most have considered islands of no more than a few tens of atoms [2,3]. For such small sizes, the details of the geometry of the structure and the many energy barriers for single-atom diffusion significantly affect the diffusion process, complicating the analysis. Recently, however, there have been two studies [4,5] in which the diffusion constant of the islands D_c was measured as a function of large approximate island radius R. Morgenstern *et al.* (MRPC) [4] have studied single-layer vacancy clusters on Ag(111). Wen *et al.* (WCBET) [5] have studied adatom islands of Ag on Ag(001). In both experiments the number of vacancies (atoms) in the island ranged from 10^2 to 10^3. For such sizes it becomes meaningful to describe the step edge position by a continuous variable. This Letter shows how the same processes that govern continuous step fluctuations also produce adatom and vacancy cluster diffusion. These equilibrium fluctuations of steps on vicinal surfaces have been observed and analyzed in detail [6–8]; specifically, their spatial and temporal correlations have been characterized in the continuum limit using Langevin dynamics [9–11]. From the similar Langevin analysis of islands that follows, we show how the Brownian motion of clusters is directly related to the various mechanisms of atomic transport across the surface. By comparison with experiment, we check that this unification of coarse-scale and atomic motion presents a self-consistent picture that is fuller than the one obtained by scaling arguments [4,5,12] alone.

Consider an adatom or vacancy island whose center of mass undergoes some random fluctuations. We assume that these fluctuations are caused entirely by the fluctuations of the boundary of the island, defined in cylindrical coordinates by

$$r = \tilde{r}(\theta, t), \tag{1}$$

where r and θ are the usual radial and azimuthal coordinates and t is the time variable. We assume that the boundary fluctuates around a fixed mean radius R. Under these conditions we can define a dimensionless variable $g(\theta, t)$ for the island boundary by

$$g(\theta, t) = [\tilde{r}(\theta, t) - R]/R. \tag{2}$$

The diffusion constant D_c of the *c*luster is defined as

$$D_c \equiv \frac{\langle \vec{\mathbf{r}}_{\mathrm{CM}}^2(t) \rangle}{4t}, \tag{3}$$

where $\vec{\mathbf{r}}_{\mathrm{CM}}(t)$ is the position vector of the center of mass of the island, and $\vec{\mathbf{r}}_{\mathrm{CM}}(0)$ is taken as the origin.

There is a close relationship between the microscopic mechanisms of mass transport and the Langevin equations that follow from them [9–11,13]. This analysis for step fluctuations of straight steps can be generalized to a circular geometry [14]. This can be shown to yield a Langevin equation for $g(\theta, t)$ of the form

$$\frac{\partial g(\theta, t)}{\partial t} = \mathcal{F}(g, \theta, t) + \zeta(\theta, t), \tag{4}$$

where $\mathcal{F}(g, \theta, t)$ is a functional of g, θ, and t, and $\zeta(\theta, t)$ is a noise term. Reminiscent of capillary-wave analysis of step motion [10,11,15], this analysis is simplified in the Fourier representations $g(\theta, t) = \sum_n g_n(t) \exp(in\theta)$, $\zeta(\theta, t) = \sum_n \zeta_n(t) \exp(in\theta)$, with $n = 0, \pm 1, \pm 2, \ldots$. Then

$$\frac{\partial g_n(t)}{\partial t} = -\tau_n^{-1} g_n(t) + \zeta_n(t). \tag{5}$$

Here τ_n is the relaxation time of an excitation of the nth mode, with wavelength $2\pi R/n$, of the cluster boundary. These relaxation times have been measured, for example, for steps on Si(111) and Si(001) [8]. From the equipartition of energy among the capillary modes $g_n(t)$, it follows that

$$\langle |g_n(t)|^2 \rangle = k_B T / 2\pi \tilde{\beta} R n^2 \tag{6}$$

in equilibrium [15], where k_B is the Boltzmann constant, T is the absolute temperature, and $\tilde{\beta}$ is the step edge stiffness.

Combining the definition (3) for D_c with Eqs. (2), (5), and (6), and linearizing in g, we get

$$D_c = k_B TR/\pi\tilde{\beta}\tau_1 . \tag{7}$$

As in the case of "straight" steps (or the decay of surface profiles [16]), there are three possibilities for the functional $\mathcal{F}$ (or the linear coefficient τ_n^{-1}) and the noise ζ, corresponding to three distinct mechanisms of mass transport occurring at the island boundary [14]. These are illustrated schematically in Fig. 1. The expressions for τ_n^{-1} can be drawn from the Langevin analyses of straight steps [10,11] essentially by substituting into the analogous expressions $|n|/R$ for the wave vector q along the step [14].

Periphery or edge diffusion (PD).—When the mass transport occurs only along the edge of the boundary (and the number of atoms or vacancies in the island are preserved), τ_n^{-1} is given by

$$\tau_n^{-1} = D_{st} c_{st} \Omega^2 \tilde{\beta} n^4 / k_B TR^4 , \tag{8}$$

where D_{st} is the (tracer) diffusion constant of a single atom diffusing along a step edge, c_{st} is the line concentration of atoms along the step edge, and Ω is the area of the surface unit cell.

Terrace or surface diffusion (TD).—Suppose that the boundary of the island can emit atoms very rapidly, but atoms can only slowly diffuse away from the boundary. The rate limiting step in mass transport is then the diffusion on terraces. We find

$$\tau_n^{-1} = 2D_{su} c_{su} \Omega^2 \tilde{\beta} |n|^3 / k_B TR^3 , \tag{9}$$

where D_{su} is the (tracer) diffusion constant of a single adatom on a flat step-free surface; c_{su} is the surface concentration of adatoms on the surface far away from the step edge in the case of an adatom island. In the case of a vacancy cluster, c_{su} is the average surface concentration of adatoms in the interior of the monolayer vacancy island.
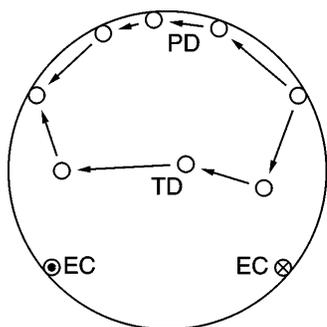
FIG. 1. Schematic representation of the three types of diffusion mechanisms considered here. The large circle represents a vacancy island on the surface. Two paths of the adatom motion marked TD (for terrace diffusion) and PD (for periphery diffusion) for the same initial and final positions of the migrating atom are depicted with arrows. The atoms marked EC represent the third mechanism of evaporation and condensation from the vacancy edge. The atom marked by a cross is one that has just condensed onto the vacancy edge. The one with a filled circle on it is the one that will soon evaporate from the edge.

Furthermore, if carriers attach or detach from only one side, as is believed to be the case for Ag(111) [4], one must remove the factor of 2 in Eq. (9).

Evaporation and condensation limited diffusion (EC).—In this case the rate limiting step for mass transport is the random attachment or detachment of adatoms (or vacancies) at the edge of the boundary (from or to a reservoir of adatoms on the terraces, or in principle in the vapor). Then τ_1 takes the form

$$\tau_n^{-1} = \Gamma\tilde{\beta} n^2 / k_B TR^2 , \tag{10}$$

where Γ, the step mobility, is proportional to the rate of random attachments (detachments) [8,15].

The cases PD, TD, and EC are examples of models B, C, and A, respectively, in dynamical critical phenomena [17]. In all three cases the diffusion constant D_c of the island or cluster is given, for small values of the time, by a relation of the form

$$D_c = D_{c0} R^{-\alpha} , \tag{11}$$

where $\alpha = 3$, 2, and 1 for the cases of PD, TD, and EC, respectively, and the corresponding expressions for D_{c0} are $D_{st} c_{st}\Omega^2/\pi$, $2D_{su} c_{su}\Omega^2/\pi$, and Γ/π. Gruber [18] found an expression for D_c for a three-dimensional void diffusing in a solid for the case of PD. Generalizing his arguments to two dimensions, we obtained the same expression for D_c as in our Langevin analysis of the PD case. To our knowledge, the expressions for TD and EC are new.

These results clearly show that the exponent α is a signature of the microscopic mechanisms of mass transport involved in the diffusion of the island. To check that these continuum results apply for the island sizes of the experiments, we also performed Monte Carlo simulations of three simple lattice-gas models corresponding to the three types of mass transport. We used the Metropolis algorithm on a square lattice with an attractive nearest-neighbor (NN) energy ϵ. Vacancy clusters with initially square shapes of linear dimension L were simulated (so $R = L/\sqrt{\pi}$). Data were not taken until the cluster had equilibrated to a nearly circular shape. In all three models L was chosen to be 10, 20, 40, and 80 atomic spacings.

In the model for PD, Kawasaki dynamics (i.e., single-atom hops to a neighboring [vacant] site) was used with the restriction that adatoms were allowed to diffuse only along the edge of the island via next-nearest-neighbor (NNN) exchange between a vacancy and an adatom. The temperature was set at $T = 0.6\epsilon/k_B$. For present purposes we define an isolated adatom (vacancy) site as one that has all four NN sites empty (occupied by atoms). On a perfectly straight step, a NN hop of an edge atom causes the formation of an isolated vacancy and an isolated adatom. This process costs an energy 6ϵ and hence is very slow. If the isolated adatom now hops along the edge to remove the isolated vacancy-adatom pair just generated, then it can do so with unit probability since the energy cost is $-\epsilon$. However, if the isolated adatom

created does not hop along the edge before the vacancy penetrates the bulk, then we get bulk vacancy diffusion, which is prohibited in PD. (If an isolated vacancy were created, its hops in the surrounding area would happen with unit probability since they involve no energy change.) Also, most atoms on an equilibrated vacancy-island edge can make NNN hops—but not NN hops—without generating an isolated vacancy. The exclusively NNN-hop dynamics avoids these problems of very slow PD diffusion with NN hops and penetration of isolated vacancies into the bulk [19]. Any NNN hop that creates an isolated vacancy is also forbidden. So long as the diffusion is restricted to the periphery and is local, the exponent α should be independent of the specific choice of dynamics.

In the model for TD, the lattice-gas Hamiltonian was slightly modified so that the energy of an isolated adatom on the terrace within the vacancy island was assigned an energy of ϵ rather than 4ϵ, increasing the equilibrium adatom density to about 10%. This modification allows the vacancy cluster edge to emit atoms rapidly, thereby facilitating adatom motion across the pit. Kawasaki dynamics was again used, but now diffusion of adatoms was allowed only via nearest-neighbor exchange between a vacancy and an adatom. The temperature was set at $T = 0.5\epsilon/k_B$.

In the model for EC, Glauber dynamics (i.e., removal or addition of single atoms) was used with random attachment or detachment of adatoms allowed only along the edge of the island, at $T = 0.6\epsilon/k_B$. In this dynamics the number of vacancies in the cluster fluctuates. For each value of L, the chemical potential of the reservoir was adjusted so that the mean number of vacancies comprising the cluster remained approximately the same as in the initial square configuration.

From the vacancy island simulations, plots of $\log D_c$ vs $\log L$ were made in all three cases. These plots with their best linear fits are shown in Fig. 2. The slopes of the linear fits gave the three values of $\alpha = 3.1$, 2.03, and 0.97, respectively. These values confirm the predictions of the Langevin analysis and the correspondence of the mass-transport mechanisms with the different values of α. The y intercepts of these fits gave the values of D_{c0}, which in turn give D_{st}, D_{su}, and Γ in the three cases.

In each case, to check the derived value of D_{c0}, we computed using the same Hamiltonians and dynamics, but applying a weak potential gradient $\mathbf{F}$ in various ways, the constituent diffusion constant, D_{st}, D_{su}, or Γ/a (where a is a lattice constant along the step). The average velocity $\bar{\mathbf{v}}$ of the diffusing species was calculated as a function of $\mathbf{F}$, and the carrier diffusion constant obtained by applying the Einstein-Nernst relation $D = k_B T|\bar{\mathbf{v}}|/|\mathbf{F}|$. For PD $\mathbf{F}$ was applied along (parallel to) the initial straight edge of a step of width $w = 40$. For the TD case $\mathbf{F}$ was applied along one direction of a flat step-free square terrace with an adatom density c_{su}. For EC $\mathbf{F}$ was applied perpendicular to an initial straight step of width
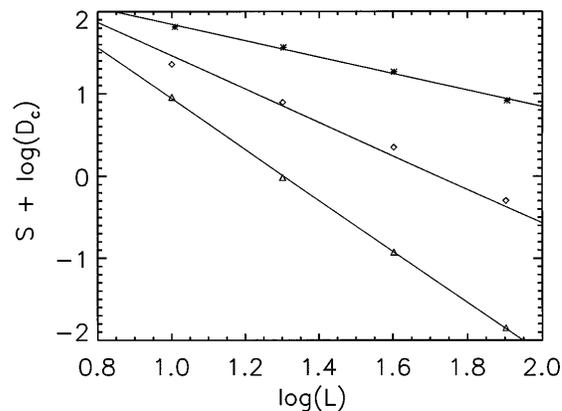
FIG. 2. Plot of $\log(D_c)$ vs $\log(L)$ obtained from simulations of the three cases: EC (asterisks), TD (diamonds), and PD (triangles) is shown along with the best linear fits. $L = R\sqrt{\pi}$ is the linear dimension of the initial square shape of the vacancy. D_c is the diffusion constant of the cluster defined by Eq. (3). The arbitrary term S shifts the y intercepts to allow display of all three cases together.

$w = 40$. In this case $\bar{\mathbf{v}}$ refers to the average velocity of the whole step. The three diffusion constants D_{st}, D_{su}, and Γ/a calculated from the set of simulations with $\mathbf{F}$ agreed to within 25% with their values obtained from the y intercepts (D_{c0}) in Fig. 2. The vacancy islands are finite in size and hence have a nonzero curvature of their boundaries even when they are perfectly circular (i.e., even when $g = 0$). Also the Langevin analysis was done only to first order in g. Considering this finite size effect of the simulations and the linear approximation in the Langevin approach we see that the agreement between diffusion constants obtained in the two ways is good. This agreement shows that the Langevin analysis gives a good description of the simulations.

The area fluctuations appear to be crucial to obtain $\alpha = 1$. In a separate simulation, we modified the TD program so that atoms were removed from one position along the boundary and immediately reattached to it elsewhere [so that area is conserved: $\oint \zeta(\theta, t) d\theta = 0$]. The resulting log-log plot indicated $\alpha = 1.97$. In fact, this scenario might better describe the diffusion of clusters on terraces with low diffusion barriers (especially close-packed faces). For adatom islands (but not vacancy pits) another diffusion mechanism is possible on such faces, e.g., on {111} fcc or hcp faces with adsorption in either threefold site. Here diffusion can occur rapidly by the passage through the island of a dislocation line between domains in each of the two kinds of sites [20].

For PD diffusion WCBET [5] cite values of α from different simulations [21,22] in the range of 3 to 4. In these simulations the number of single atoms or vacancies in the islands were less than 10^2. We believe that these values should converge to $\alpha = 3$ for larger island sizes. WCBET [5] also present heuristic arguments for obtaining the value of α for EC and PD diffusion. Stimulated by the work of Pimpinelli et al. [23], MRPC [4] give

a similar explanation of the phenomenon. Though this approach predicts the correct exponents for the PD and TD mechanisms of diffusion, it does not readily provide precise quantitative information, such as the single-atom diffusion constants and the step stiffness.

This Letter demonstrates that the phenomenon of surface diffusion of large islands can be viewed in a broader perspective: the cluster diffusion is a natural by-product of the fluctuations of the bounding step. Observations of step fluctuations can then be used to make predictions about island diffusion. This approach also gives quantitative predictions for tracer diffusion constants from the observations of large island diffusion, as we illustrate for the two experiments at hand. Using $D_c \approx 0.1$ Å^2/s for an adatom island of 100 atoms on Ag(001) from WCBET [5], we get $\Gamma/a \approx 1.8$ Å^2/s for the diffusion of a step on Ag(001) at room temperature. Approximating the diffusion prefactor by 10^{13} Å^2/s [2], we obtain an activation energy of ≈ 0.7 eV, which is a reasonable magnitude for a single atom detaching from a close-packed step. From MRPC [4] we use $D_{c0} \approx 1.3 \times 10^4$ Å^4/s to get the surface mass diffusion coefficient of Ag adatoms on Ag(111), $D_{su}c_{su} \approx 750$ s^{-1}. Using an upper limit of 0.01% (1%) adatom density in the pit, we get a lower limit for D_{su} of 5×10^7 (10^5) Å^2/s. With the prefactor 10^{13} Å^2/s [2], we get an upper limit for the activation energy for an atom to diffuse on a Ag(111) terrace of about 0.3 (0.4) eV, again of a plausible order of magnitude.

In conclusion, a Langevin analysis of diffusion of large islands has been developed. With Monte Carlo simulations we have illustrated the predictions of the analysis for surface mass transport. This approach allows us to measure single-adatom diffusion constants from observations of large island diffusion.

[1] J. J. Métois, K. Heinemann, and H. Poppa, Philos. Mag. **35**, 1413 (1977).

[2] G. L. Kellogg, Phys. Rev. Lett. **73**, 1833 (1994); Surf. Sci. Rep. **21**, 1 (1994).

[3] S. C. Wang and G. Ehrlich, Surf. Sci. **239**, 301 (1990).

[4] K. Morgenstern, G. Rosenfeld, B. Poelsema, and G. Comsa, Phys. Rev. Lett. **74**, 2058 (1995).

[5] J. M. Wen, S.-L. Chang, J. W. Burnett, J. W. Evans, and P. A. Thiel, Phys. Rev. Lett. **73**, 2591 (1994).

[6] L. Kuipers, L. M. S. Hoogeman, and J. W. M. Frenken, Phys. Rev. Lett. **71**, 3517 (1993).

[7] M. Poensgen, J. F. Wolf, J. Frohn, M. Giesen, and H. Ibach, Surf. Sci. **274**, 430 (1992).

[8] N. C. Bartelt, J. L. Goldberg, T. L. Einstein, E. D. Williams, J. C. Heyraud, and J. J. Métois, Phys. Rev. B **48**, 15 453 (1993); N. C. Bartelt, R. M. Tromp, and E. D. Williams, Phys. Rev. Lett. **73**, 1656 (1994).

[9] J. Villain, J. Phys. I (France) **1**, 19 (1991).

[10] N. C. Bartelt, J. L. Goldberg, T. L. Einstein, and E. D. Williams, Surf. Sci. **273**, 252 (1992).

[11] N. C. Bartelt, T. L. Einstein, and E. D. Williams, Surf. Sci. **312**, 411 (1994).

[12] K. Binder and M. H. Kalos, J. Stat. Phys. **22**, 363 (1980).

[13] W. W. Mullins, J. Appl. Phys. **28**, 333 (1957); **30**, 77 (1959).

[14] S. V. Khare, N. C. Bartelt, and T. L. Einstein (to be published).

[15] P. Nozières, in *Solids Far From Equilibrium,* edited by C. Godrèche (Cambridge University Press, Cambridge, 1992).

[16] H. P. Bonzel and E. Preuss, Surf. Sci. **336**, 209 (1995).

[17] P. C. Hohenberg and B. I. Halperin, Rev. Mod. Phys. **49**, 435 (1977).

[18] E. E. Gruber, J. Appl. Phys. **38**, 243 (1967).

[19] This dynamics also avoids the anomalous behavior at corners in a NN-hop dynamics on a square lattice. J. G. McLean, B. H. Cooper, and E. Chason, Bull. Am. Phys. Soc. **40**, 598 (1995).

[20] J. C. Hamilton, M. S. Daw, and S. M. Foiles, Phys. Rev. Lett. **74**, 2760 (1995).

[21] H. C. Kang, P. A. Thiel, and J. W. Evans, J. Chem. Phys. **93**, 9018 (1990).

[22] A. F. Voter, Phys. Rev. B **34**, 6819 (1986); SPIE Modeling of Optical Thin Films **821**, 214 (1987).

[23] A. Pimpinelli, J. Villain, D. E. Wolf, J. J. Métois, J. C. Heyraud, I. Elkinani, and G. Uimin, Surf. Sci. **295**, 143 (1993).